JPE 18-2-25

https://doi.org/10.6113/JPE.2018.18.2.604
ISSN(Print): 1598-2092 / ISSN(Online): 2093-4718

Synchronous Carrier-based Pulse Width Modulation Switching Method for Vienna Rectifier

Jin-Hyuk Park*, SongHee Yang*, and Kyo-Beum Lee†

†,*Department of Electrical and Computer Engineering, Ajou University, Suwon, Korea

Abstract

This paper proposes a synchronous switching technique for a Vienna rectifier that uses carrier-based pulse width modulation (CB-PWM). A three-phase Vienna rectifier, similar to a three-level T-type converter with three back-to-back switches, is used as a PWM rectifier. Conventional CB-PWM requires six independent gate signals to operate back-to-back switches. When internal switches are operated synchronously, only three independent gate signals are required, which simplifies the construction of gate driver circuits. However, with this method, total harmonic distortion of the input current is higher than that with conventional CB-PWM switching. A reactive current injection technique is proposed to improve current distortion. The performance of the proposed synchronous switching method and the effectiveness of the reactive current injection technique are verified using simulations and experiments performed with a set of Vienna rectifiers rated at 5 kW.

Key words: Current distortion near the zero-crossing point, Reactive current injection method, Synchronous switching method, Vienna rectifier

I. INTRODUCTION

Environmental pollution is an important issue that has increased interest in the use of electric and hybrid electric vehicles as technologies for ecological conservation. The supply of electric vehicles decreases the global demand for oil, which creates additional economic benefits by reducing fuel costs [1]-[3]. The Vienna rectifier is typically used in electric vehicles [4]-[6].

Non-generative-boost voltage-source pulse width modulation (PWM) rectifiers that are connected to the grid with a unity power factor are known as Vienna rectifiers [7]-[9]. Vienna rectifiers are efficient three-level converters that help reduce the total harmonic distortion (THD) of input currents compared with two-level converters [10]-[12]. Moreover, Vienna rectifiers are used in various applications, such as wind turbine systems and telecommunication power systems [8]-[11], [13]-[15]. The topology of the Vienna rectifier is similar to a general three-level T-type converter (Fig. 1). The number of power devices is decreased by replacing the external switches with diodes.

Unidirectional Vienna rectifiers have a phase difference between the current and the reference voltage because of the filter impedance and power factor of the rectifier. The direction of the phase current and the reference voltage of a Vienna rectifier should be the same to avoid phase current distortion near the zero-crossing point [16].

PWM has been the subject of intensive research in power electronics and is widely employed to control power converters. A variety of modulation techniques have been studied to improve the performance of Vienna rectifiers in a range of applications. Hysteresis is a switching method that can control the input current as a sinusoidal waveform [17]. This method has variable switching frequency through the operation of the reference current and the hysteresis band. The hysteresis method guarantees fast dynamic response, but achieving the optimal design of the input filter is difficult. Constant switching frequency is used in carrier-based PWM (CB-PWM). Sinusoidal modulating signals in CB-PWM are compared with triangular carrier signals to generate the output voltage. An advantage of the carrier-based switching method is its ability to obtain the duration of active and zero vectors easily. This method needs two independent modulation signals to operate the back-to-back switch of each phase.

The various switching methods of the Vienna rectifier have

Manuscript received Jun. 30, 2017; accepted Nov. 21, 2017
Recommended for publication by Associate Editor Liqiang Yuan.
†Corresponding Author: kyl@ajou.ac.kr
Tel: +82-31-219-2376, Fax: +82-31-219-9531, Ajou University
*Dept. of Electrical and Computer Engineering, Ajou University, Korea

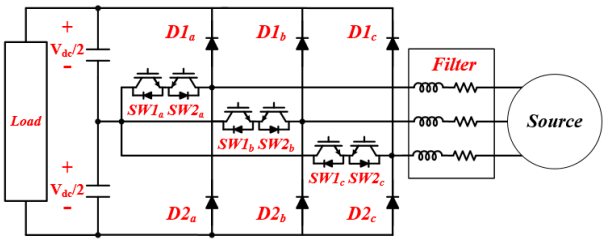

Fig. 1. Topology of the Vienna rectifier.

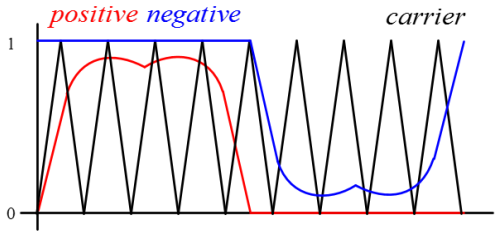

Fig. 2. Modulation signals for the CB-PWM.

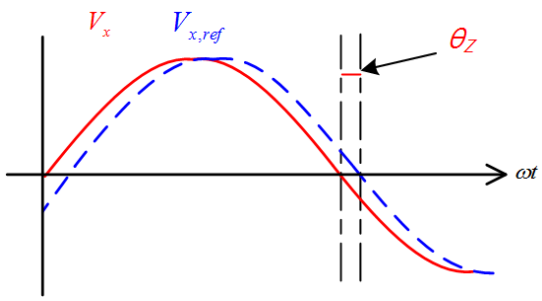

Fig. 3. Impedance angle of the Vienna rectifier.

been studied [16], [18]-[20]. A discontinuous conduction mode (DCM) control with light load conditions is proposed in [18]. The currents are distorted because the relationship between the average half-bridge voltage and the duty cycle becomes nonlinear. The sampled currents are also not equal to the average currents. The present study analyzes the current patterns according to the switching states and calculates the duty cycles for DCM to achieve sinusoidal currents. However, this method is difficult to implement because many cases have the current patterns and the calculation of DCM duty cycles is complicated. The CB-PWM method for a variable power factor is proposed in [16]. This switching method adds the compensation voltage to the three-phase reference voltage for the variable power factor without current distortion. However, the region where the compensation is possible is limited by the modulation index. The new CB-PWM switching method for a discontinuous PWM (DPWM) is proposed in [19]-[20] and is implemented in a similar way as in [16]. In the region where the requirement is violated, the reference voltage is settled to zero by adding the offset voltage. The zero clamping region is expanded as the modulation index decreases. Much of the harmonic voltages are generated and increases the THD of the current.

Two devices are in the same state (ON or OFF) when the back-to-back switches are operated synchronously. An advantage of the proposed method over the conventional CB-PWM is that the number of modulation signals is halved. Therefore, the volume and cost of the power converter can be reduced because the gate driver circuit is simplified. Vienna rectifiers are generally operated in a continuous conduction mode. However, the current cannot flow to the neutral point when the back-to-back switches are turned off near the zero-crossing point. Thus, a different current path is generated compared with the path generated using the conventional CB-PWM. Therefore, in this region, a DCM is initiated, and DCM switching states are added [21]. Thus, input currents around the zero-current point are more distorted with this method compared with the conventional CB-PWM [22].

This study proposes a synchronous CB-PWM switching method. When internal switches are synchronized, the number of modulation signals can be reduced by half. As a result, costs are reduced with the proposed CB-PWM method because only half the gate driver circuits are used. However, an algorithm is necessary to improve the current quality because current distortion with the proposed switching method is worse if no algorithm is applied at the zero-crossing point. The optimal reactive current is injected to solve this distortion problem. The effectiveness of the proposed switching method is demonstrated using PSIM simulations and experiments.

II. General Vienna Rectifier

The topology of the Vienna rectifier is shown in Fig. 1. The Vienna rectifier consists of three back-to-back switches, six diodes, and a grid-connected L-filter. The modulation signals of a three-level system are illustrated in Fig. 2, in which each phase has two modulation signals: a positive modulation signal and a negative modulation signal. The positive and negative modulation signals are used to control SW2 and SW1, respectively. SW1 maintains the ON state when SW2 is triggered. Conversely, SW2 maintains the ON state when SW1 is triggered.

Positive and negative modulations are used for each phase. Thus, a three-phase Vienna rectifier requires six modulation signals. With a Vienna rectifier, the sign of the input current should also correspond to the sign of the reference voltage (V_{x_ref}). The quality of the current depends on whether this requirement is satisfied in all phases. The quality of the current depends on whether this requirement is satisfied in all phases. The grid current is distorted (Fig. 3) if the requirement is unsatisfied around the zero-crossing point because of filter impedance. The phase difference between the grid current and V_{x_ref}, which is caused by a delay due to the filter impedance, is called the impedance angle (θ_z). V_{x_ref}

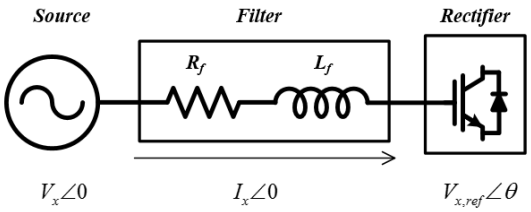

Fig. 4. Equivalent circuit of the Vienna rectifier.

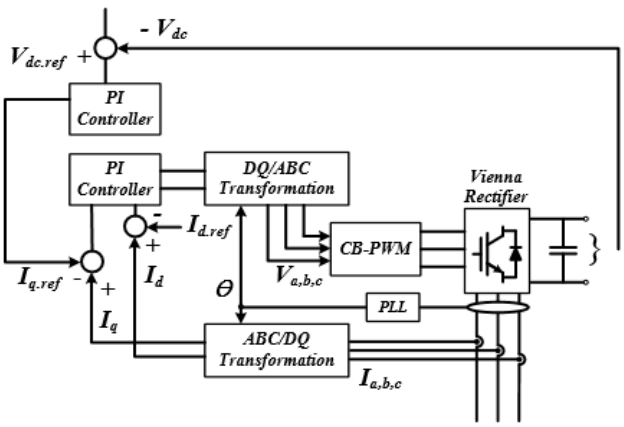

Fig. 5. Block diagram of the control scheme for the Vienna rectifier.

must have a phase of θ_z in reference to the grid voltage (V_x) to control the grid current as a sinusoidal waveform. The phase difference between V_{x_ref} and the grid current (I_x) is treated as θ_z when Vienna rectifiers are operated with a unity power factor because I_x and V_x share the same phase.

Fig. 4 illustrates the equivalent circuit of the Vienna rectifier. The phases of V_x and I_x are the same in the unity power factor condition. V_x_ref has a phase of θ_z in reference to V_x. This study only considers the resistor and filter inductor in calculating θ_z. The voltage equation for Fig. 4 can be indicated as

$$V_{x,ref}\angle\theta_Z = (V_x - R_f I_x) - j2\pi f_s L_f I_x, \quad (1)$$

where R_f is the resistance, f_s is the line frequency, and L_f is the filter inductance.

Equation (1) can be rearranged as

$$\tan\theta_Z = \frac{-2\pi f_s L_f I_x}{V_x - R_f I_x}. \quad (2)$$

With Equation (2), θ_z can be calculated as

$$\theta_Z = \tan^{-1}\left(\frac{-2\pi f_s L_f I_x}{V_x - R_f I_x}\right). \quad (3)$$

θ_Z can be calculated as the filter impedance for the grid voltage at unity power factor. This study uses Equation (3) in the reactive current injection algorithm.

A double control loop is typically used to control the Vienna rectifier. This control scheme is shown in Fig. 5. The outer loop is a DC voltage controller to regulate the DC voltage.

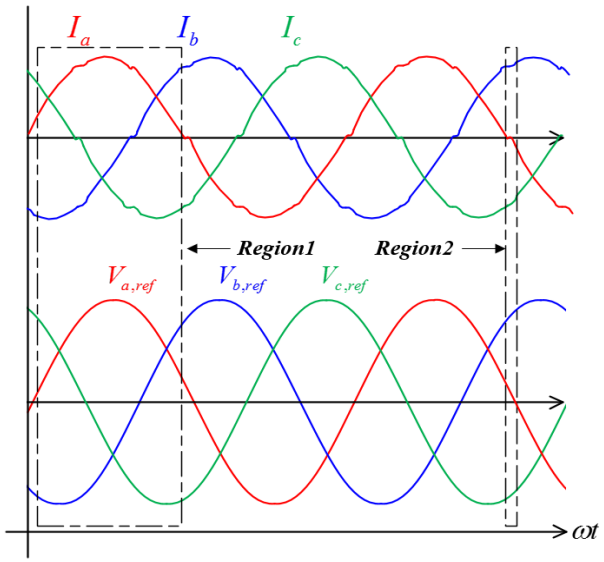

Fig. 6. Currents and reference voltages for CB-PWM.

A current controller is used in the inner loop to control the power factor and amplitude of the input current. The current controller can be implemented in a synchronous coordinate frame. The synchronous angle is estimated using a phase lock loop to transform the coordinate frame. Reference voltages obtained by the current controller are used to generate the PWM signals.

III. Proposed Synchronous CB-PWM Switching Method

With conventional CB-PWM, one back-to-back switch is clamped to the ON state, while the other switch is triggered during a half period of the grid voltage. Thus, the states of the power devices are switched independently of each other, and the conventional CB-PWM method requires six modulation signals. This study proposes that the back-to-back switches are operated synchronously, and only three modulation signals are required with this method. The back-to-back switches are triggered simultaneously when the proposed technique is used. Thus, the number of gate driver circuits and the cost and size of the system can be reduced.

A. Conventional CB-PWM Switching Method

When the CB-PWM method is used with a Vienna rectifier, an offset voltage (V_{offset}) is added to the three-phase reference voltage ($V_{x,ref} = V_{a,ref} = V_{b,ref} = V_{c,ref}$) to expand the modulation index. V_{offset} is calculated as

$$\begin{aligned} V_{a,reft} &= V_m \sin(\omega t) \\ V_{b,reft} &= V_m \sin(\omega t - 2\pi/3) \\ V_{c,reft} &= V_m \sin(\omega t + 2\pi/3) \end{aligned} \quad \text{and} \quad (4)$$

$$V_{offset} = \frac{V_{\max} + V_{\min}}{2}, \quad (5)$$

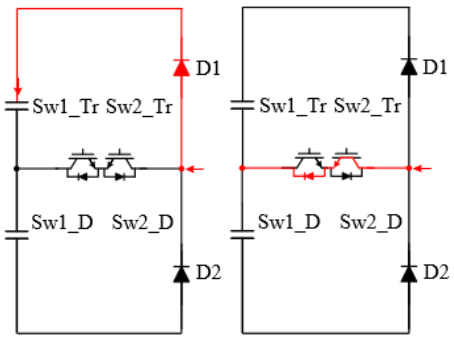

(a) SW1 : ON, SW2 : OFF (P State) (b) SW1 : ON, SW2 : ON (O state)

Fig. 7. Current flow in Region 1 with conventional CB-PWM.

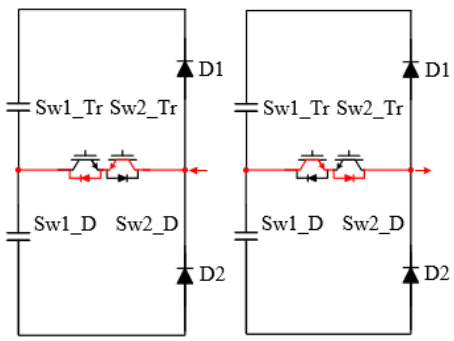

(a) (b)

Fig. 8. Current flow in Region 2 with the conventional CB-PWM switching method. (a) SW1: ON, SW2: ON (O State). (b) SW1: ON, SW2: OFF (O state).

where V_m is the magnitude of the reference voltage, V_{max} is the maximum voltage, and V_{min} is the minimum voltage of $V_{x,ref}$.

This study adds the reference voltage when the offset voltage ($V_{x,ref,offset}$) is calculated as

$$V_{x,ref,offset} = V_{x,ref} + V_{offset}. \quad (6)$$

Fig. 6 shows the reference voltages and grid currents of the rectifier. The requirement that the direction of the phase current and the reference voltage of the Vienna rectifier are the same is satisfied in Region 1. Fig. 7 shows the current path in Region 1 according to switching state. SW2 is toggled between the ON and OFF states. SW1 is clamped to the ON state when $V_{a,ref}$ is positive. As the current flows through the neutral point, the switching state is O when SW2 is ON. With the current flowing through D1, the switching state is P when SW1 is ON.

θ_z is the phase difference between the current and the reference voltage of the Vienna rectifier. This phase difference is used to define Region 2, where θ_z is not as stated. Deviation from the definition of θ_z leads to distortions of the currents around the zero-crossing point. Fig. 8 shows the current path in Region 2 according to the switching state. SW1 is clamped to the ON state because $V_{a,ref}$ remains positive. The current flows through the neutral point and the switching state is maintained at O regardless of the switching state of SW2. Fig. 9 shows the sequence of the voltage vector in this region.

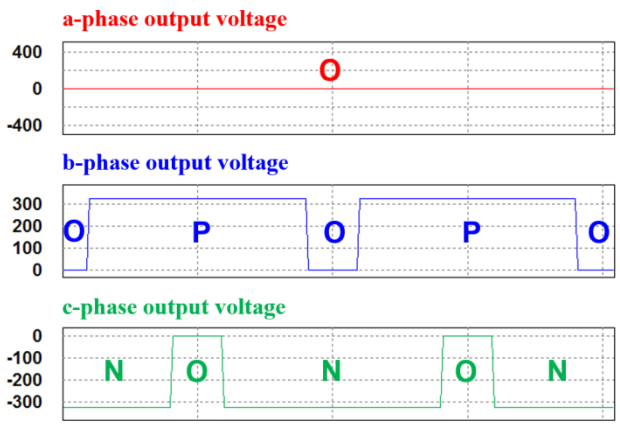

Fig. 9. Output voltages of the rectifier and corresponding switching states in Region 2 with the conventional CB-PWM switching method.

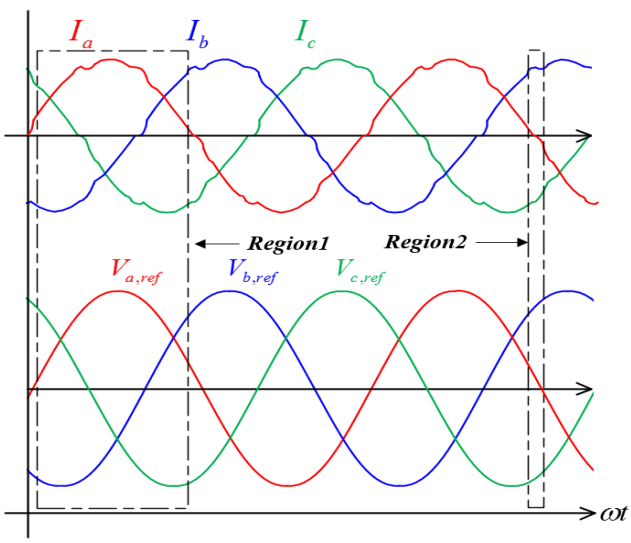

Fig. 10. Currents and reference voltages for the synchronous CB-PWM.

B. *Proposed Synchronous CB-PWM Switching Method*

The reference voltages for the proposed CB-PWM switching method are used in the same way as for the conventional CB-PWM method.

The grid currents and reference voltages are shown in Fig. 10. The requirement on the sign of the input current and voltage reference is satisfied in Region 1. When SW1 and SW2 are turned on at the same time, current flows through the neutral point and the switching state is O. When SW1 and SW2 are turned off at the same time, the current flows through D1 and the switching state is P. The current path is as depicted in Fig. 7 when the proposed switching method is used in Region 1. Consequently, the performance of the

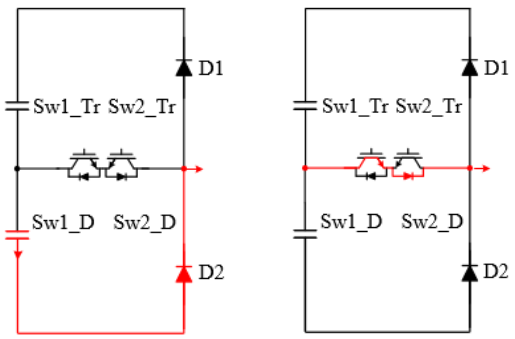

Fig. 11. Current flow in Region 2 with the proposed CB-PWM switching method. (a) SW1: OFF, SW2: OFF (N State). (b) SW1: ON, SW2: ON (O state).

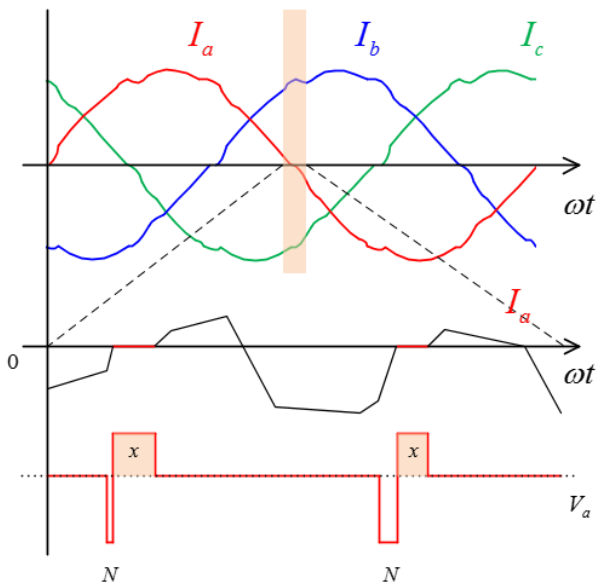

Fig. 12. Voltage and input currents of the rectifier during DCM.

Vienna rectifier is the same regardless of the switching method.

The current path in Region 2 for the proposed CB-PWM switching method is shown in Fig. 11. The switching state is as depicted in Fig. 8(b) when both switches are ON. Therefore, the current flows through the neutral point, and the switching state is O. However, the current path to the neutral point is blocked when SW1 and SW2 are turned off, and different voltage vectors are injected, as shown in Fig. 11(a). These conditions cause a voltage error between the output voltage and the reference voltage. Current distortion is thus worse at the zero-crossing point due to the voltage error. When both switches are OFF, current flows through D2 and the switching state becomes N [Fig. 11(a)]. The current rapidly decreases to zero in this switching state. No current flows, and the DCM is initiated after the current reaches zero (Fig. 12). Fig. 12 shows the input currents and the associated voltages at DCM to illustrate the additional switching state. These switching states adversely affect the current quality

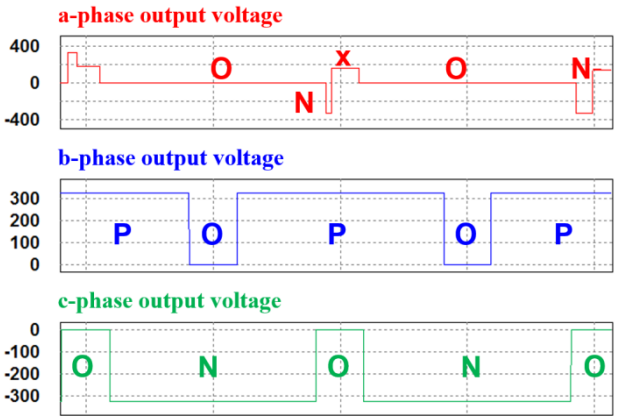

Fig. 13. Output voltages of the three phases in Region 2 with the proposed CB-PWM method.

TABLE I
SI BASE POSSIBLE WITCHING STATES IN DCM

No.	DCM	DCM used in this paper
1	xPO	O
2	PxO	X
3	xNO	O
4	NxO	X
5	OPx	X
6	OxP	O
7	ONx	X
8	OxN	O
9	POx	O
10	xOP	X
11	NOx	O
12	xON	X
SUM	12	6

unlike those depicted in Fig. 9. The additional switching states from the DCM are listed in Table I. "x" indicates that no current flows in the related phase. The number of possible switching states in one-phase DCM is 12. The voltage vectors injected by DCM depend on the phase of the reference voltage. With the proposed switching method, DCM is found at the right side of the zero-crossing point of the current because $V_{x,ref}$ lags the current by the impedance angle. Therefore, this study only uses half of the possible 12 voltage vectors introduced by DCM. Fig. 13 shows the applied voltage vector sequence in Region 2. The [NPO] and [xPO] voltage vectors are additional and unnecessary compared with the voltage vectors depicted in Fig. 9. These unnecessary voltage vectors further distort the current around the zero-current point in each phase.

C. Improvement Algorithm of the Current Distortion

Here, we propose a reactive (d-axis) current injection technique to improve grid current distortion. The Vienna rectifier is operated in a non-unity power factor condition.

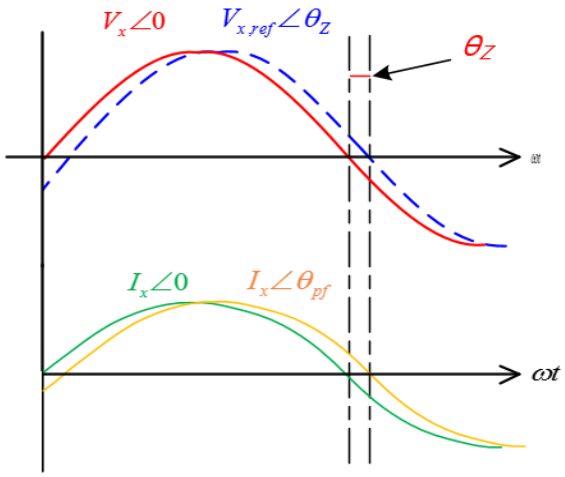

Fig. 14. Phase differences depending on the impedance angle and power factor angle.

When injecting the d-axis current, a phase difference called the power factor angle (θ_{pf}) occurs. Current distortion can be improved by compensating θ_{pf} for θ_Z.

In the non-unity condition, the power factor can be classified as either the leading power factor or the lagging power factor, depending on the phases of the grid current and the grid voltage. Fig. 14 shows the phase differences between the current and the reference voltage depending on the impedance angle and the power factor angle. $V_{x,ref}$ is separated by θ_Z, as shown in Fig. 14. To compensate for θ_Z, a lagging power factor angle is selected. $V_{x,ref}$ and I_x indicate the same phase when the optimal d-axis current is injected. In this case, the requirement is satisfied in the overall region, and the current distortion problem in Region 2 can be solved.

Therefore, θ_{pf} should be obtained using the same value as θ_Z for calculating the optimal reactive current. θ_{pf} can be obtained simply using Ide and I_{qe} as [17]:

$$\theta_{pf} = \cos^{-1}\left(\sqrt{\frac{I_{qe}^2}{I_{de}^2 + I_{qe}^2}}\right). \tag{7}$$

First, θ_{pf} should be obtained from $\sin(\theta_{pf})$ by injecting the appropriate d-axis current. If θ_{pf} is sufficiently small, then $\sin(\theta_{pf})$ can be approximated to θ_{pf}. In the range where θ_{pf} is between 0° and 20°, $\sin(\theta_{pf})$ is approximated to θ_{pf} within 2% error. In the experimental conditions, the maximum value of θ_Z is roughly 7° so θ_{pf} can be estimated within 1% error. Therefore, the influence of the estimation error on (9) is extremely small. On the basis of (7) and (8), θ_{pf} can be expressed as

$$\sin\theta_{pf} = \sqrt{1-\cos^2\theta_{pf}}. \tag{8}$$

$$\sin\theta_{pf} \approx \theta_{pf} = \sqrt{\frac{I_{de}^2}{I_{de}^2 + I_{qe}^2}}. \tag{9}$$

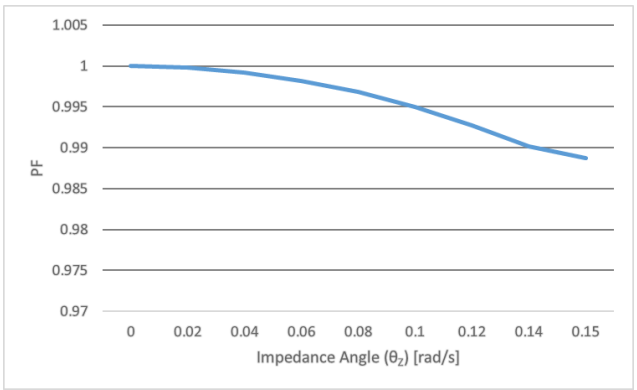

Fig. 15. Power factor based on impedance angle.

Assuming that θ_Z and θ_{pf} are the same, I_{de} can be calculated as

$$I_{de} = \sqrt{\frac{I_{qe}^2\theta_Z^2}{1-\theta_Z^2}}. \tag{10}$$

When (10) is used, the optimal reactive current can be injected, thereby reducing the current distortion.

In case the reactive current is injected, when substituting (10) into (7), θ_{pf} can be represented by only θ_Z. θ_{pf} is expressed as

$$\theta_{pf} = \cos^{-1}\left(\sqrt{1-\theta_Z^2}\right). \tag{11}$$

Following (11), the power factor is also represented by θ_Z.

$$\sqrt{1-\theta_Z^2} = \cos\left(\theta_{pf}\right). \tag{12}$$

The power factor depending on θ_Z is shown in Fig. 15, where 0.15 rad/s in the x-axis corresponds to 10°. The power factor decreases as θ_Z increases. θ_Z consistently exists in the Vienna rectifier and is affected by the filter inductance and the grid current. In the experimental condition, the maximum value of θ_Z is approximately 0.12 rad/s at the rated power.

The power factor of the proposed algorithm is slightly lower than that of the conventional CB-BPWM because of the injection of the reactive current. However, the magnitude of the reactive current is small compared with that of the active current. Thus, the Vienna rectifier can control the power factor to near unity. The distortion of the grid current is likewise reduced without a large change in the power factor.

The information of the power factor and the impedance angle must be used to implement the proposed algorithm. Here, we consider the fundamental component. The power factor can be simply approximated by (7) with the active and reactive currents, which are calculated by the sampled grid current. The impedance angle can be also obtained by the filter inductor and the sampled grid voltage and current. When harmonic currents occur because of the distorted grid voltage, an error occurs in the calculated power factor angle and impedance angle. This error can be reduced by using the

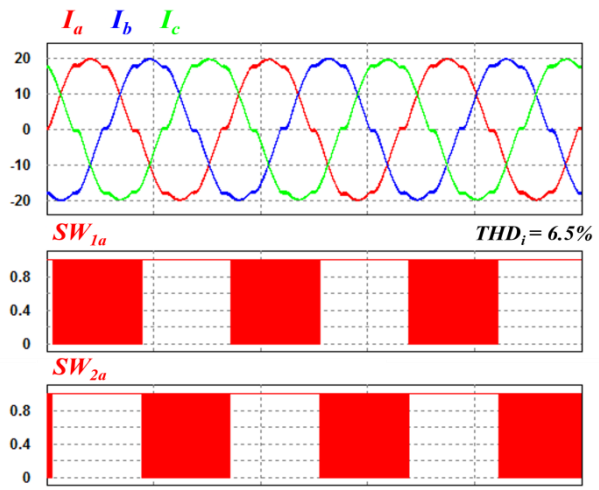

Fig. 16. Simulated currents and switching signals for the conventional CB-PWM.

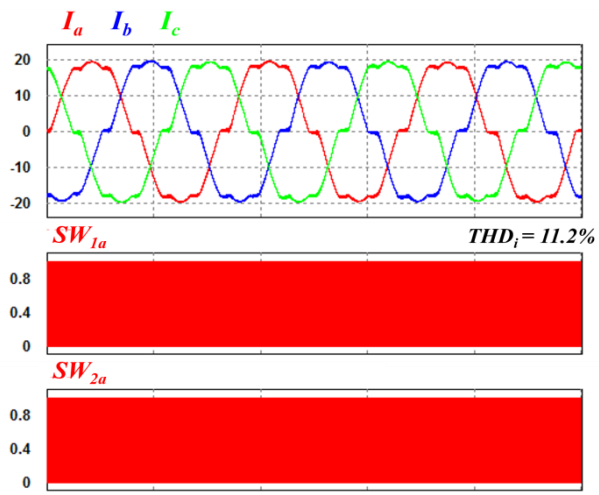

Fig. 17. Simulated currents and switching signals for the synchronous CB-PWM.

TABLE II
SIMULATION PARAMETER

Parameter	Value
Line-to-line voltage	220 $V_{ll,rms}$
Line frequency	60 Hz
Filter inductance (L_f)	3.5 mH
Filter resistance (R_f)	0.5 Ω
DC-link voltage	450 V
DC-link capacitor	550 uF
Rated power	5 kW
Switching frequency	10 kHz
Control period	100 us

digital low pass filter on DSP, because the grid voltage and current used in the calculation appear as DC components when only the fundamental components are considered.

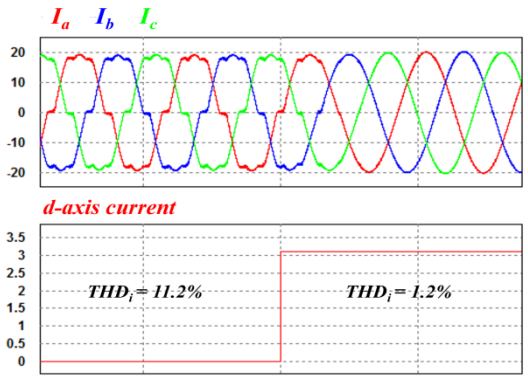

Fig. 18. Results of simulations performed using the proposed algorithm for improving current distortion.

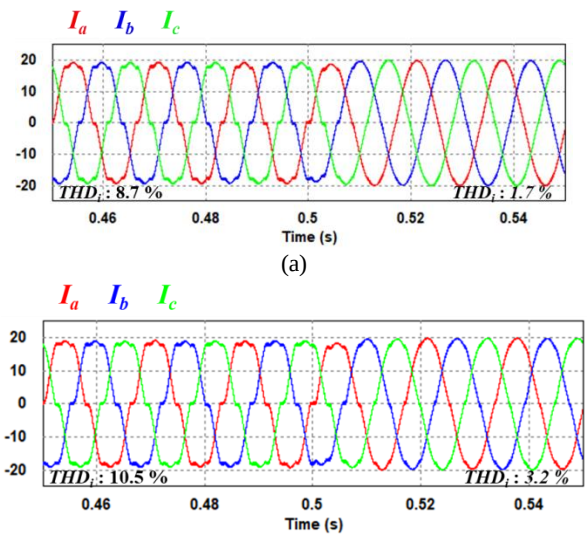

Fig. 19. Performance of the proposed method under distorted voltage. (a) 5th: 3%, 7th: 2%. (b) 5th: 5%, 7th: 3%.

IV. SIMULATION RESULTS

Simulations were implemented using a PSIM tool to demonstrate the effectiveness of the synchronous CB-PWM technique with the algorithm for improving current distortion for a Vienna rectifier. The simulation parameters are listed in Table II. The circuit used in the simulation is depicted in Fig. 1.

The simulated grid currents and switching signals of the a-phase when the conventional CB-PWM technique is used are presented in Fig. 16. The switching signals are asynchronous, and the input currents are distorted near the zero-current point when the relevant requirement is not satisfied, as shown in the figure. THDi is approximately 6.5%.

The simulation results of the synchronous CB-PWM switching method are shown in Fig. 17. The switching signals are synchronous, and SW1 and SW2 are switched simultaneously. In comparison with the results depicted in Fig. 16, the grid currents around the zero crossing are more

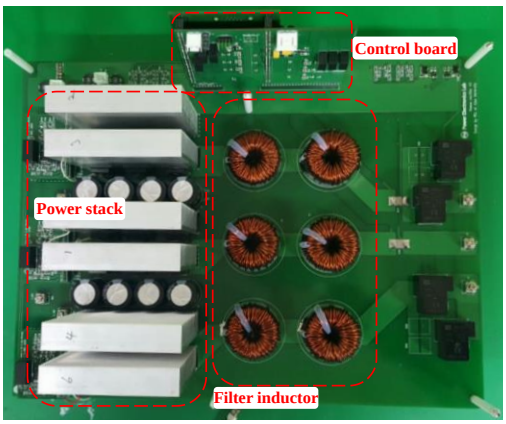

Fig. 20. Prototype of a Vienna rectifier used in the experiments.

distorted because of the injection of the unnecessary voltage vectors. THDi increases to 11.2%.

The effectiveness of the proposed algorithm for improving current distortion seen with the synchronous CB-PWM switching method is shown in Fig. 18. The distortion of the grid currents is reduced by injecting the optimal reactive current, thereby equalizing the phase of the current and the reference voltage (Fig. 14). In the rated power condition, the q-axis current is 20 A and the d-axis current is 2.5 A. The magnitude of the reactive current is extremely small compared with the active current. Consequently, the power factor is controlled to near unity. In addition, THDi is approximately 1.2%, which is an approximate 10% improvement compared with the results in Fig. 17.

The current distortion under the distorted grid voltage is shown in Fig. 19. The conventional CB-PWM switching method is used before 0.5 s, and the proposed switching method with the optimal reactive is applied after 0.5 s. To simulate the distorted grid, we add the fifth and seventh harmonic voltages, which are injected with a ratio based on the magnitude of the grid voltage, to the simulation condition. Before 0.5 s, THDi is increased compared with that in Fig. 16 because of the distorted voltage. When the proposed method is used, THDi drastically decreases after 0.5 s. However, the current distortion by the distorted voltage remains, though the current distortion by the proposed switching method and impedance angle disappears, as shown in Fig. 19. Therefore, the THDi of Fig. 19 is higher than that of Fig. 18.

V. Experiment Results

This section presents the results of experiments conducted to verify the performance of the proposed synchronous CB-PWM switching method with an optimal reactive current injection to improve current quality. The parameters of the experiment are the same as the simulation parameters listed in Table II.

Experiments were conducted using a set of prototypes of a Vienna rectifier rated at 5 kW (Fig. 20). The prototype consists

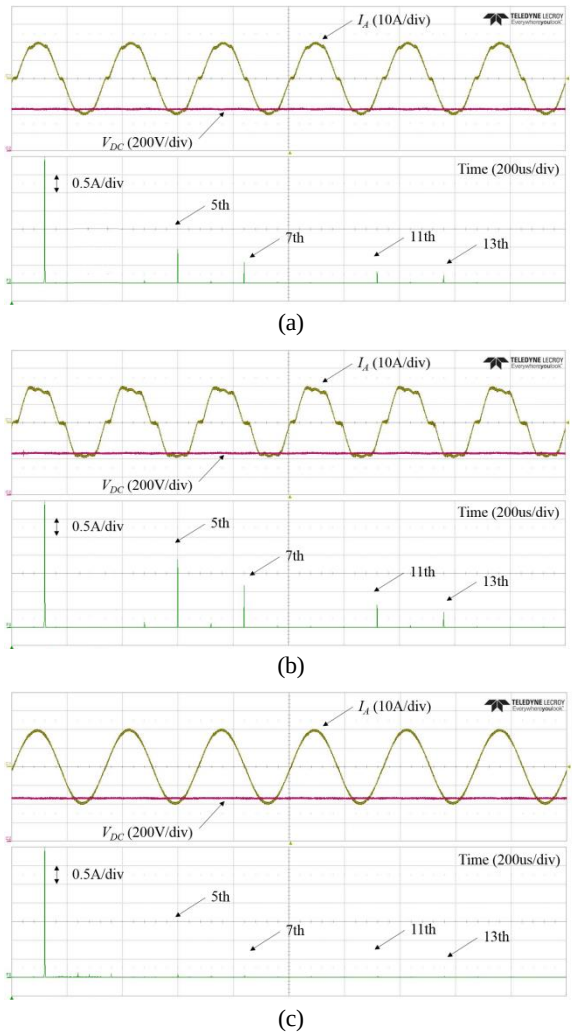

Fig. 21. Experiment results in the rated load condition. (a) Conventional CB-PWM. (b) Proposed synchronous CB-PWM. (c) Proposed synchronous CB-PWM and optimal reactive current injection.

of a control board, a power board, and filter inductors. A digital signal processor (TMS320F28335 DSP) is used in the control board. The power board comprises the rectifier and the filter inductor. The THD and power factor of the current were measured using a WT3000 power analyzer.

The experimental results at rated power conditions are shown in Fig. 21. Under these conditions, the Vienna rectifier controls the DC-link voltage to 450 V. The performance of the conventional CB-PWM is presented in Fig. 21(a). Distortion of the input current occurs at the zero-crossing point, and lower order harmonics such as the 5th, 7th, 11th, and 13th appear, as shown in the fast Fourier transform in Fig. 21(a). These results are similar to those in the simulations. THDi is approximately 6.6%.

The results of experiments conducted with the proposed CB-PWM technique are shown in Fig. 21(b). When the proposed synchronous CB-PWM switching method is applied, unnecessary voltage vectors are injected in the region in

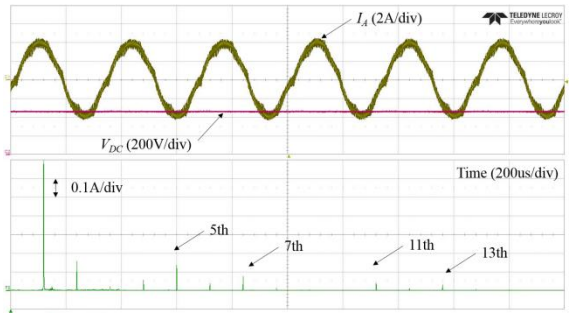

(a)

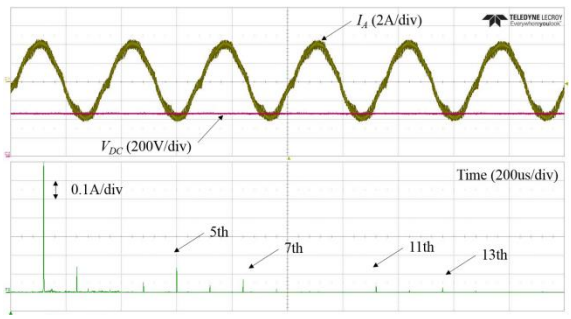

(b)

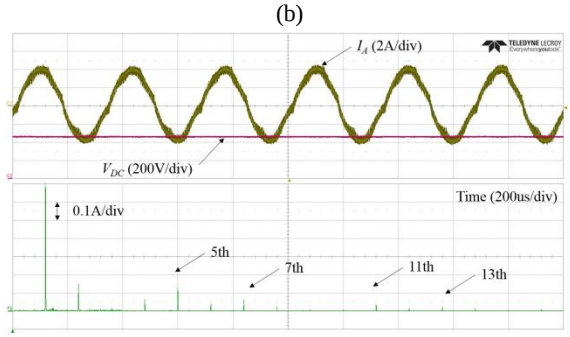

(c)

Fig. 22. Experiment results in 1 kW load condition. (a) Conventional CB-PWM. (b) Proposed synchronous CB-PWM. (c) Proposed synchronous CB-PWM and optimal reactive current injection.

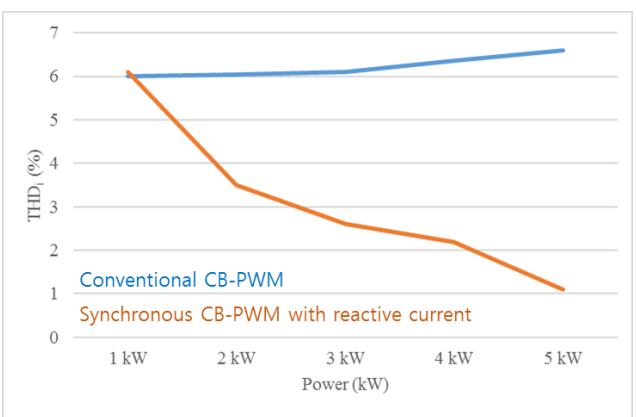

Fig. 23. Variation of THDi based on switching methods.

which the direction of the current and voltage of the rectifier is different. These voltage vectors increase the distortion of the input current at the zero-crossing point. The magnitudes

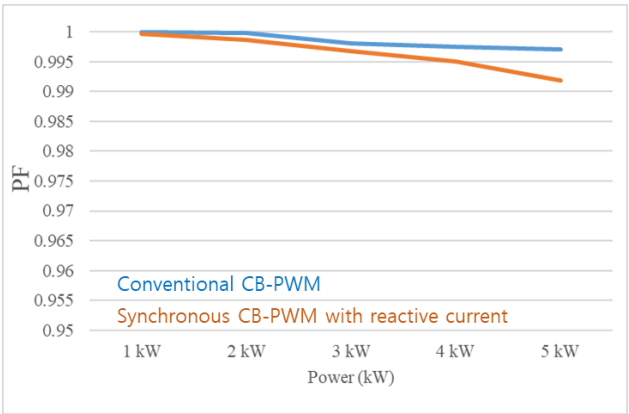

Fig. 24. Variation of power factor based based on switching methods.

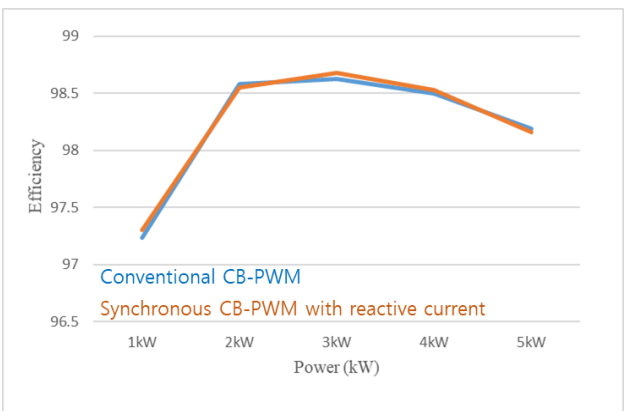

Fig. 25. Efficiency according to switching methods.

of the 5th, 7th, 11th, and 13th harmonics, as shown in Fig. 21(b), are larger than those in Fig. 21(a). Therefore, THDi increases to 12.8% compared with the results depicted in Fig. 21(a).

The performance of the current injection technique with synchronous CB-PWM is shown in Fig. 21(c). The magnitudes of the 5th, 7th, 11th, and 13th harmonics are reduced and current distortion around the zero-crossing point is improved compared with the results shown in Figs. 21(a) and 21(b). THDi is approximately 1.1%, which is a 5% improvement compared to Fig. 21(a). We inject an optimal reactive current of 2.5 A to improve current quality. Given that the magnitude of the reactive current is extremely small compared with the active current (20 A), the Vienna rectifier can control the power factor to almost unity. Hence, the power factor is measured as 0.991 by the power analyzer, which is extremely close to a unity power factor.

The results of experiments conducted at 1 kW load condition are shown in Fig. 22. Other experimental conditions are the same as those used to obtain the results in Fig. 21. The distortion of the current at the zero-crossing point is similar with that in Figs. 22(a), (b), and (c), unlike the results in Fig. 21. In light load conditions, θ_Z is extremely small, such that the region in which the unnecessary voltage vectors are

injected is narrow. Therefore, the current distortion at the zero-crossing point is not severe. In Fig. 22(a), θ_Z is approximately 1.3°. To compensate for θ_Z, 0.1 A reactive current is injected [Fig. 22(c)]. When comparing the THDi of Figs. 22(a) and (c), the results are similar by approximately 6%.

Experiments between 1 and 5 kW were also conducted to verify the proposed control method with the entire load. Current distortion depends on the magnitude of the input current, as described by (3). The magnitude of THDi based on the variation of the load is illustrated in Fig. 23. In the light load condition, current distortion is not severe regardless of the switching method because the impedance angle is extremely small, as dictated by (3). Therefore, the THDi of both switching methods are similar. As the load increases, the THDi of the conventional CB-PWM also increases because of the larger impedance angle. When the proposed synchronous CB-PWM algorithm is used, THDi decreases as the load increases because, as shown in Fig. 21(c), the magnitudes of the lower order harmonics are reduced by injecting the optimal reactive current. Therefore, the quality of the input current improves compared with that of the conventional CB-PWM.

The power factor based on the variation of the load is illustrated in Fig. 24. The optimal reactive currents are 0.10, 0.40, 0.91, 1.61, and 2.53 A per additional 1 kW load. The optimal reactive current is injected as the load current varies. The magnitude of the reactive current is small compared with the active current of the entire load. θ_Z increases with the load, as shown in (3). The magnitude of the optimal reactive current also increases, thereby improving the current distortion, and it is determined by (10). The power factor decreases as θ_Z increases, as shown in (12). Therefore, the power factor of the high power condition is lower than that of the light power condition. The results show that the power factor decreases as the load increases (Fig. 24). However, the power factor is above 0.99 for all considered loads. Consequently, the Vienna rectifier can control the power factor to almost unity.

The efficiency based on the switching methods is shown in Fig. 25. In the conventional CB-PWM, one of the back-to-back switches is triggered and the other is clamped to the ON state during a half period of the grid voltage. By contrast, in the proposed method, the back-to-back switches are operated synchronously. The switching number of the proposed method is twice as large as that of the conventional CB-PWM during a period of the grid voltage. However, in the almost region, the current path is the same as that in Fig. 7 regardless of the switching methods. When using the proposed switching method, in a switch in which current flows through anti-parallel diode, switching loss does not occur. Therefore, the mechanism of the power loss is the same as that for both switching methods. The experimental results indicate that the efficiency of both switching methods is similar for the entire load.

VI. Conclusions

We proposed a synchronous CB-PWM switching method for the Vienna rectifier with an algorithm to improve current distortion. The Vienna rectifier typically requires six modulation signals if the conventional CB-PWM method is used. With the proposed synchronous CB-PWM method, the number of modulation signals is reduced to three from six. Therefore, reducing the cost and volume of the system is possible by using simplified gate driver circuits. However, when this method is applied, unnecessary voltage vectors are generated because of DCM, and currents are distorted around the zero-crossing point. A representative THDi of 6.6% was observed with the conventional CB-PWM switching method; this value increased to 12.8% with the proposed CB-PWM switching method at the rated power condition. Here, we proposed an optimal reactive current injection technique to improve current distortion. The optimal reactive current can be obtained simply based on the system parameters using the power factor angle and impedance angle. When this technique was used, the THDi was improved to 1.2%. Thus, the power factor can be controlled to above 0.99 because the magnitude of the injected reactive current is extremely small compared with the active current. The effectiveness of the proposed synchronous CB-PWM method with the reactive current injection algorithm was verified via PSIM simulation and experiments.

Acknowledgment

This work was supported by the Korea Institute of Energy Technology Evaluation and Planning (KETEP) and the Ministry of Trade, Industry & Energy (MOTIE) of the Republic of Korea (No. 20171210201100 and No. 20174030201660).

References

[1] J. S. Park, M. J. Kim, H. S. Jeong, J. H. Kim, and S. W. Choi, "Development of 50kW high efficiency modular fast charger with wide charging voltage range," *Trans. Korean Inst. Power Electron.*, Vol. 21, No. 3, pp. 267-274, Jun. 2016.

[2] A. Ansari, P, Cheng, and H.-J. Kim, "A 3 kW bidirectional DC-DC converter for electric vehicles," *J. Electr. Eng. Technol.*, Vol. 11, No. 4, pp. 860-868, Jul. 2016.

[3] S. G. Farkoush, C.-H. Kim, H.-C. Jung, S. Lee, N. T. Umpon, and S.-B. Rhee, "Power factor improvement of distribution system with EV chargers based on SMC method for SVC," *J. Electr. Eng. Technol.*, Vol. 12, No. 4, pp. 860-868, Jul. 2017.

[4] S. Yang, J.-H, Park, and K.-B. Lee, "Current quality improvement for a Vienna rectifier with high-switching frequency," *Trans. Korean Inst. Power Electron.*, Vol. 22, No. 2, pp. 181-184, Apr. 2017.

[5] A. K. Yadav, P. Gaur, S. K. Jha, J. R. P. Gupta, and A. P. Mittal, "Optimal speed control of hybrid electric vehicles," *J. Power Electron.*, Vol. 11, No. 4, pp. 393-400, Jul. 2011.

[6] A. Ghaderi, T. Umeno, Y. Amano, and S. Masaru, "A novel seamless direct torque control for electric drive vehicles," *J. Power Electron.*, Vol. 11, No. 4, pp. 449-455, Jul. 2011.
[7] N. T. B. Soeiro and J. W. Kolar, "Analysis of high-efficiency three-phase two- and three-level unidirectional hybrid rectifiers," *IEEE Trans. Ind. Electron.*, Vol. 60, No. 9, pp. 3589-3601, Sep. 2013.
[8] M. S. Ortmann, S. A. Mussa, and M. L. Heldwein, "Three-phase multilevel PFC rectifier based on multistate switching cells," *IEEE Trans. Power Electron.*, Vol. 30, No. 4, pp. 1843-1854, Apr. 2015.
[9] T. Friedli, M. Hartmann, and J. W. Kolar, "The essence of three-phase PFC rectifier systems – Part II," *IEEE Trans. Power Electron.*, Vol. 29, No. 2, pp. 543-560, Feb. 2014.
[10] A. Rajaei, M. Mohamadian, and A. Y. Varjani, "Vienna-rectifier-based direct torque control of PMSG for wind energy application," *IEEE Trans. Ind. Electron.*, Vol. 60, No. 7, pp. 2919-2929, Jul. 2013.
[11] H. Chen and D. C. Aliprantis, "Analysis of squirrel-cage induction generator with VIENNA rectifier for wind energy conversion system," *IEEE Trans. Energy Convers.*, Vol. 26, No. 3, pp. 967-975, Sep. 2011.
[12] J.-S. Lee, E. S. Lee, and K.-B. Lee, "Hybrid parallel three-level converter topology for large wind turbine generation systems," in *Proc, ISIE*, pp. 515–520, 2014.
[13] B. Kedjar, H. Y. Kanaan, and K. A. Haddad, "Vienna rectifier with power quality added function," *IEEE Trans. Ind. Electron.*, Vol. 61, No. 8, pp. 3847-3856, Aug. 2014.
[14] J. Adhikari, P. IV, and S. K. Panda, "Reduction of input current harmonic distortions and balancing of output voltages of the Vienna rectifier under supply voltage disturbances," *IEEE Trans. Power Electron.*, Vol. 32, No. 7, pp. 5802-5812, Jul. 2017.
[15] L. Hang, H. Zhang, S. Liu, X. Xie, C. Zhao, and S. Liu, "A novel control strategy based on natural frame for Vienna-type rectifier under light unbalanced-grid conditions," *IEEE Trans. Ind. Electron.*, Vol. 62, No. 3, pp. 1353-1362, Mar. 2015.
[16] J.-S. Lee and K.-B. Lee, "A novel carrier-based PWM method for vienna rectifier with a variable power factor," *IEEE Trans. Ind. Electron.*, Vol. 63, No.1, pp. 3-12, Jan. 2016.
[17] A. Rajaei, M. Mohamadian, and A. Y. Varjani, "Vienna-rectifier-based direct torque control of PMSG for wind energy application," *IEEE Trans. Ind. Electron.*, Vol. 60, No. 7, pp. 2919-2929, Jul. 2013.
[18] M. Leibl, J. W. Kolar, and J. Deuringer, "Sinusoidal input current discontinuous conduction mode control of the Vienna rectifier," *IEEE Trans. Power Electron.*, Vol. 32, No. 11, pp. 8800-8812, Nov. 2017.
[19] J.-S. Lee and K.-B. Lee, "Carrier-based discontinuous PWM method for vienna rectifiers," *IEEE Trans. Power Electron.*, Vol. 30, No. 6, pp. 2896-2900, Jun. 2015.
[20] J.-S. Lee and K.-B. Lee, "Performance analysis of carrier-based discontinuous PWM method for Vienna rectifiers with neutral-point voltage balance," *IEEE Trans. Power Electron.*, Vol. 31, No. 6, pp. 4075–4084, Jun. 2016.
[21] P. Ide, F. Schafmeister, N. Fröhleke and H. Grotstollen, "Enhanced control scheme for three-phase three-level rectifier at partial load," *IEEE Trans. Ind. Electron.*, Vol. 52, No. 3, pp. 719-726, Jun. 2005.
[22] S. Yang, J.-H, Park, and K.-B. Lee, "A carrier-based PWM with synchronous switching technique for a Vienna rectifier," in *Proc. PECON*, pp. 728-733, 2016.

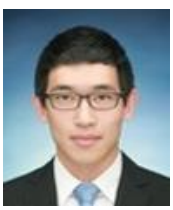

Jin-Hyuk Park received his B.S. degree in Electronic Engineering from Ajou University, Suwon, Korea in 2013. He is presently working toward his Ph.D. degree in Electronic Engineering at Ajou University. His current research interests include power conversion and grid-connected systems.

SongHee Yang received her B.S. and M.S degree in Electronic Engineering from Ajou University, Suwon, Korea in 2012 and 2017, respectively. Her current research interests include power conversion and grid-connected systems.

Kyo-Beum Lee received his B.S. and M.S. degrees in Electrical and Electronic Engineering from Ajou University, Suwon, Korea, in 1997 and 1999, respectively. He received his Ph.D. degree in Electrical Engineering from Korea University, Seoul, Korea, in 2003. From 2003 to 2006, he was with the Institute of Energy Technology, Aalborg University, Aalborg, Denmark. From 2006 to 2007, he was with the Division of Electronics and Information Engineering, Chonbuk National University, Jeonju, Korea. In 2007, he joined the School of Electrical and Computer Engineering, Ajou University. He is an Associate Editor of the IEEE Transactions on Power Electronics, the Journal of Power Electronics, and the Journal of Electrical Engineering and Technology. His current research interests include electric machine drives, renewable power generation, and electric vehicle applications.